Lidocaine Induces Apoptosis in Head and Neck Squamous Cell Carcinoma Cells Through Activation of Bitter Taste Receptor T2R14

Zoey A. Miller,[1,2] Jennifer F. Jolivert,[1] Ray Z. Ma,[3] Sahil Muthuswami,[1] Arielle Mueller,[1] Derek B. McMahon,[1] Ryan M. Carey,[1] & Robert J. Lee[1,4,5]

[1]Department of Otorhinolaryngology, University of Pennsylvania Perelman School of Medicine, Philadelphia, PA
[2]Pharmacology Graduate Group
[3]Harriton High School, Bryn Mawr, PA
[4]Department of Physiology, University of Pennsylvania Perelman School of Medicine, Philadelphia, PA
[5]Correspondance to: rjl@pennmedicine.upenn.edu

Abstract

Head and Neck Squamous Cell Carcinomas (HNSCCs) have high mortality due to late stage diagnosis, high metastasis rates, and poor treatment options. Current therapies are invasive and aggressive, leading to a severe decline in patient quality of life (QoL). It is vital to create new therapies that are both potent and localized and/or targeted to prolong survival while maintaining QoL. Lidocaine is a local anesthetic used in HNSCC surgery settings. Lidocaine also activates bitter taste (taste family 2) receptor 14 (T2R14). T2Rs are G-protein coupled receptors (GPCRs) that increase intracellular Ca^{2+} when activated. T2Rs are expressed in mucosal epithelia, including internal regions of the head and neck, and are accessible drug targets. Here, we show that lidocaine increases intracellular Ca^{2+} and decreases cAMP in several HNSCC cell lines. Ca^{2+} release from the ER results in Ca^{2+} uptake into the mitochondria. Ca^{2+} mobilization is blocked with GPCR inhibitors and T2R14 antagonists. Lidocaine activation of T2R14 depolarizes the mitochondrial membrane, inhibits cell proliferation, and induces apoptosis. Lidocaine activates caspase-3 and -7 cleavage and also increases total caspase protein levels despite no changes in mRNA production. Both total and cleaved caspase products were upregulated even in the presence of cycloheximide, an inhibitor of protein synthesis. This suggests inhibition of the ubiquitin-proteasome system. It is vital to understand Lidocaine-induced apoptosis in HSNCCs to utilize its chemotherapeutic effects as a treatment option. In addition, future studies on T2R14 expression in HNSCC patients could provide insight for implementing lidocaine as a targeted topical therapy.

Keywords: G protein-coupled receptor, calcium, cyclic-AMP, anesthetic, chemosensory receptor

Introduction

Head and Neck Squamous Cell Carcinomas (HNSCCs) arise in the oral and nasal cavities, larynx, and pharynx, typically as a result of exposures to environmental carcinogens and/or human papilloma virus [1-4]. HNSCCs account for 600,000 cancer diagnoses per year, with a 5-year mortality rate of ~50% [5-7]. This due to frequrent late-stage diagnoses and/or lack of preventive screening. They also have high rates of metastasis [8-10]. Surgical resection is a first line treatment but is aggressive and invasive, leaving with patients with a severe decrease in quality of life (QoL) [3]. These patients can lose the ability to orally communicate or ingest food, have altered taste perception, be prone to asphyxiation, have exterior malformations, and more [11, 12]. In addition to the lasting effects of surgery, HNSCC patients also experience the generalized side effects of combined radiation and/or chemotherapy [13]. The only FDA-approved targeted therapy for HNSCCs is epidermal growth factor receptor (EGFR) inhibitor cetuximab. However, cetuximab still does not differentiate between normal and cancerous tissue [14]. It is vital to develop novel targeted therapies to maintain QoL while undergoing treatment and to prolog survival for HNSCC patients.

A majority of HNSCC cases are localized to the oral cavity [15]. A main function of this region is human taste perception. Humans can perceive five main “flavors”: sour, salty, sweet, umami, and bitter [16]. Sour and salty flavors are perceived through the activation of ion channels, whereas sweet, umami, and bitter flavors are perceived through the activation of GPCRs [17-21]. This stimulates the production of secondary messengers to release neurotransmitters from taste bud cells to nearby gustatory nerves [22, 23]. GPCR taste receptors are classified into two groups: taste family 1(T1Rs; sweet and umami) and taste family 2 (T2Rs; bitter) [24]. While there are only 3 isoforms of T1Rs, there are 25 T2R isoforms in humans [25], which function to protect against ingestion of bitter tasting toxins [26]. The canonical T2R signaling pathway is an intracellular calcium (Ca^{2+}) increase and cyclic adenosine monophosphate (cAMP) decrease [27]. The Ca^{2+} response is through activation of PLCβ2 via Gβγ subunits of the G-protein heterotrimer [28-30], which produces inositol triphosphate (IP_3) and stimulates the release of Ca^{2+} from the endoplasmic reticulum (ER) [31, 32].

GPCRs are leveraged as therapeutic targets in diseases due to their multifaceted roles in cellular functions [33]. As GCPRs, T2Rs are also being investigated for many diseases as they are expressed outside the oral cavity (extraoral) and have been associated with susceptibility to non-taste related diseases [34-36]. Beyond taste, T2Rs play roles in innate immunity, thyroid function, cardiac physiology, and more [37-41].

Extraoral T2R isoforms T2R4 and T2R14 are being investigated in cancer [42]. In models of breast, ovarian and pancreatic cancers, T2R4 and T2R14 agonists killed cancers cells, and in some cases, left normal surrounding tissue unharmed [43, 44]. We hypothesized that T2R4 and/or T2R14 agonists may have similar effects in HNSCCs. We previously showed that bitter agonists cause an increase in nuclear and mitochondrial

Ca^{2+} that leads to apoptosis in squamous de-differentiated non-ciliated airway epithelial cells [29] and HNSCC cells [45]. While we found that Ca^{2+} is required for this apoptosis, the underlying mechanisms of this T2R-induced endpoint are largely unknown despite other studies also linking T2Rs to apoptosis. Nonetheless, because many clinical drugs are bitter, we hypothesized that T2Rs in cancer cells might be targeted by already-approved bitter drugs.

Lidocaine is a commonly used as a local anesthetic in HNSCC surgery settings [46], blocking sodium (Na^{+}) channels to inhibit pain signals from sensory neurons [47]. Lidocaine may also have chemotherapeutic effects and lower rates of metastasis [48-53]. Interestingly, lidocaine is known to be bitter and may interact with heterologously-expressed T2R14 [54]. It also shares structural similarities with multi-T2R agonist denatonium benzoate. From this, we hypothesized that lidocaine might kill HSNCC cells through activation of T2R14.

Here, we show that lidocaine induces Ca^{2+} responses in HNSCC cells, and that this response is blocked by a T2R14 antagonist. Moreover, lidocaine decreases HNSCC cell viability, depolarizes the mitochondrial membrane potential, and induces apoptosis. Apoptosis is blocked by T2R14 antagonism. Interestingly, we also observe that bitter agonists lidocaine and denatonium benzoate can inhibit the proteasome, revealing another possible mechanism of T2R agonist-evoked apoptosis. Taken together, our data identify a mechanism of action of the apoptotic effects of lidocaine observed in several types of cancer cells and suggest that lidocaine may be useful to repurpose as a chemotherapeutic for HNSCCs.

Methods

Cell Culture

SCC4 (ATCC CRL-1624), SCC47 (UM-SCC-47; Millipore SCC071), SCC90 (ATCC CRL-3239), FaDu (ATCC HTB-43), RPMI 2650 (CCL-30), and HEK 293T (ATCC CRL-3216) cell lines were from ATCC (Manassas, VA, USA) or MilliporeSigma (St. Louis, MO USA). All cell lines were grown in submersion in high glucose Dulbecco's modified Eagle's medium (Corning; Glendale, AZ, USA) with 10% FBS (Genesee Scientific; El Cajon, CA, USA), penicillin/streptomycin mix (Gibco; Gaithersburg, MD, USA), and nonessential amino acids (Gibco). Stable SCC90 T2R4 siRNA knockdown cells were generated previously [45]. Unless indicated below, all reagents were from MilliporeSigma.

Quantitative reverse transcription PCR (qPCR)

Cell cultures were resuspended in TRIzol (Thermo Fisher Scientific; Waltham, MA, USA). RNA was isolated and purified (Direct-zol RNA kit; Zymo Research), reverse transcribed via High-Capacity cDNA Reverse Transcription Kit (Thermo Fisher Scientific), and quantified using TaqMan qPCR probes for *TAS2R4, CASP3, CASP7,* and *UBC* (QuantStudio 5; Thermo Fisher Scientific). *UBC* was used as an endogenous control due to its stability in expression in cancer cells [55].

Live Cell Imaging

For calcium (Ca^{2+}) imaging, cells were loaded with 5 μM of Fluo-4-AM (Thermo Fisher Scientific) for 50 min at room temperature in the dark. Hank's Balanced Salt Solution (HBSS) buffered with 20 mM HEPES (pH 7.4) was used as an imaging buffer, containing 1.8 mM Ca^{2+}. Cells were imaged using a Nikon Eclipse TS100 (20x 0.75 NA PlanApo objective), FITC filters (Chroma Technologies), QImaging Retiga R1 camera (Teledyne; Tucson, AZ, USA), MicroManager, and Xcite 120 LED Boost (Excelitas Technologies; Mississauga, Canada). For experiments in Ca^{2+}-free (0-Ca^{2+}) HBSS, cells were loaded with Fluo-4-AM as described above in normal Ca^{2+}-containing HBSS. Bitter agonists were dissolved in HBSS with no added Ca^{2+} plus 10 mM EGTA (0-Ca2+ HBSS) and was used in the place of regular HBSS (no EGTA). At the start of the experiment, 300 uL of bitter agonist in 0-Ca2+ HBSS was added to 60 uL of Ca^{2+}-containing HBSS for final concentrations of ~8.3 mM EGTA and 0.3 mM Ca^{2+} with a predicted free extracellular Ca^{2+} of 2.1×10^{-9} mM (MaxChelator, Chris Patton, Stanford University, https://somapp.ucdmc.ucdavis.edu/pharmacology/bers/maxchelator/). This method resulted in an acute removal of extracellular free Ca^{2+} at the exact time of agonist addition.

For mitochondrial and endoplasmic reticulum Ca^{2+} imaging, pcDNA-4mt3cpv or pcDNA-D1ER was transfected into cells using lipofectamine 3000 reagents (Thermo Fisher Scientific) 24-48 hours prior to imaging [56]. Live cell images were taken on

Olympus IX-83 microscope (20x 0.75 NA PlanApo objective), CFP/YFP filters (Chroma 89002-ET-ECFP/ EYFP) in excitation and emission filter wheels (Sutter Lambda LS), Orca Flash 4.0 sCMOS camera (Hamamatsu, Tokyo, Japan), Meta-Fluor (Molecular Devices, Sunnyvale, CA USA), and XCite 120 LED Boost (Excelitas Technologies).
For cyclic adenosine monophosphate (cAMP) imaging, pcDNA3.1(-)Flamindo2 was transfected into cells as described above 48 hours prior to imaging [57]. Cells were imaged as described above for mitochondrial and endoplasmic reticulum Ca^{2+} using FITC filters.
For diacylglycerol (DAG) imaging, RED Upward DAG Assay Kit (Montana Molecular; Bozeman, Montana, USA) was transduced into cells using 2x the recommended reagents. Cells were used 24 hours-post transduction and imaged as described above for mitochondrial and endoplasmic reticulum using TRITC filters. Novel T2R14 inhibitors LF1 and LF22 were identified based on a structure-search using information from and purchased from a chemical vendor (Enamine, Monmouth Jct., NJ; cat # Z85879385 and Z3906872216). Compounds were dissolved in DMSO at 500 mM and used at 1:1000 as indicated. Stock solutions were stored at -20° C [58].

Cell Viability and Proliferation

Cells were incubated with bitter agonists for 6 or 24 hours at 37 °C. Crystal violet (0.1% in deionized water with 10% acetic acid) was used to stain remaining adherent cells. Stains were washed with deionized water and left to dry at room temperature. Stains were dissolved with 30% acetic acid in deionized water. Absorbance values at 590 nm were measured. XTT dye and phenazine methosulfate were added to cells in combination with bitter agonists. Measurements were taken at 475 and 660 nm over 6 hours. Absorbance values were measured on a Tecan (Spark 10M; Mannedorf, Switzerland). Lidocaine was dissolved in Matrigel (Corning) on ice. Thin formulation was made by combining 75 µL Matrigel and 75 µL of 20 mM lidocaine. Thick formulation was made by combining 150 µL Matrigel and 150 µL of 20 mM lidocaine. The lidocaine Matrigel was added on top of cells in 8-well glass chamber slides (~0.86 cm^2 surface area per well). After 24 hours, live cell images were taken on Olympus IX-83 microscope (20x 0.75 NA PlanApo objective), Orca Flash 4.0 sCMOS camera (Hamamatsu, Tokyo, Japan), Meta-Fluor (Molecular Devices, Sunnyvale, CA USA), and Differential Interference Contrast (DIC) filter.

Mitochondrial membrane potential and apoptosis measurements

Cells were loaded with JC-1 dye for 15 minutes. Bitter agonists were added as indicated. Fluorescence was measured at 488nm excitation and 535 (green) and 590 (red) nm emission. Live cell images of the assay were taken on Olympus IX-83 microscope (20x 0.75 NA PlanApo objective), FITC and TRITC filters (Chroma Technologies), Orca Flash 4.0 sCMOS camera (Hamamatsu, Tokyo, Japan), Meta-Fluor

(Molecular Devices, Sunnyvale, CA USA), and XCite 120 LED Boost (Excelitas Technologies). Quantitative fluorescence values were measured on a Tecan Spark 10M. CellEvent Caspase 3/7 dye was added to cells in combination with bitter agonists. Fluorescence was measured at 495 nm excitation and 540 nm emission. Live cell images were taken as described above for JC-1 assays (only FITC filter). Quantitative fluorescence values were measured on a Tecan Spark 10M.

Western Blotting

Protein was harvested using lysis buffer (10 mM Tris pH 7.5, 150 mM NaCl, 10 mM KCl, 0.5% deoxycholic, 0.5% Tween, 0.5% IGePawl, 0.1% SDS). Protein content was quantified using DC Protein Assay (BioRad; Hercules, CA, USA). 50 – 80 µg of protein were loaded into gel (Bis-Tris 4-12%, 1.5 mm) with 4x loading buffer (200 mM Tris pH 6.8, 40% glycerol, 8% SDS, 0.1% Bromophenol Blue), and 5% β-mercaptoethanol. Gel was run using MES running buffer (Tris Base 50 mM pH 7.3, MES 50 mM, SDS 0.1%, EDTA 1 mM). Novex Sharp Pre-Stained Protein Standard or SeeBlue Plus2 Pre-stained Protein Standard (Thermo Fisher) were used as molecular markers. Gel was transferred using Bis-Tris transfer buffer (25 mM bicine, 25 mM bis-tris, 1 mM EDTA, 10% methanol). Blots were blocked for 1 hour in TBST (24.8 mM tris acid & base, 1.5 NaCl, 0.5% Tween-20) with 5% milk. Primary antibodies were used 1:1000 in TBST with 5% BSA. Antibodies included caspase-3 (Cell Signaling #9662), caspase-7 (Cell Signaling #9492), cyclin D1 (Cell Signaling #2978), and β-Actin (Cell Signaling #3700). HRP-conjugated chemiluminescent secondary antibodies were used 1:1000 in TBST with 5% milk (Cell Signaling anti-Rabbit or anti-Mouse Goat Horse Radish Peroxidase). Blots were imaged using Clarity Max Western ECL Substrate (BioRad) using ChemDoc MP Imaging System (BioRad).

Statistical Analysis

Data were analyzed using *t*-test (two comparisons only) or one-way ANOVA (>2 comparisons) in GraphPad Prism (San Diego, CA, USA). Both paired and unpaired *t*-test were used when appropriate. Bonferroni and Dunnett's posttest for one-way ANOVA were used when necessary. All figures used the following annotations: $P < 0.05$ (*), $P < 0.01$ (**), $P < 0.001$ (***), and no statistical significance (ns). All data points represent the mean +/- SEM.

Results

Lidocaine stimulation causes an intracellular Ca^{2+} response

T2R14 is one of the T2R isoforms most strongly expressed in extraoral tissues [59]. To understand if lidocaine can activate T2R14 in HNSCC cells, Ca^{2+} responses were recorded in living cells loaded with Fluo-4 AM in response to bitter agonists [60] (peak responses shown in Fig 1A-C). Lidocaine induced the highest Ca^{2+} response among all compounds screened (at their maximum concentrations in aqueous solution), including denatonium benzoate (non-T2R14 agonist whose Ca^{2+} response is dependent on T2R4 in these cells [45]), thujone (T2R14 agonist), flufenamic acid (T2R14 agonist), and ATP (purinergic receptor agonist) [54, 61, 62] (Fig 1A-C). Dose dependent Ca^{2+} responses were recorded with lidocaine ranging from 100 μM to 10 mM, with 10 mM evoking the highest response [63, 64] (Fig 1D & E; Supplemental Fig 1A-C). At both 5 and 10 mM, lidocaine induced higher Ca^{2+} responses than denatonium benzoate (Fig 1D-G). Denatonium benzoate is a non-T2R14 agonist that induces apoptosis in HNSCC cells and is categorized as the most bitter compound in the world because it activates eight T2R isoforms [65, 66]. In addition, 10 mM lidocaine caused a sustained heightened Ca^{2+} level post-stimulation (Fig 1E). Lidocaine also induced a higher Ca^{2+} response than a closely related local anesthetic, procaine [67], at equivalent concentrations (Supplemental Fig 1D). Procaine is not known to activate T2R14. Thus, we hypothesized that the Ca2+ response is not due to Na^{+} channel inhibition but another mechanism, possibly from intracellular sources.

Lidocaine exhausted secondary Ca^{2+} responses with ATP, used as a control due to its ability to activate intracellular Ca^{2+} responses via purinergic receptors [62]. ATP was used following lidocaine (1 – 10 mM) stimulation in SCC 4 and SCC 47 cells as Ca^{2+} levels returned to baseline. As lidocaine concentration increased, the post-ATP Ca^{2+} response decreased, suggesting immense depletion of Ca^{2+} stores by lidocaine (Fig 2A-D). Taken together, the Ca^{2+} responses observed in HNSCC cells with lidocaine indicates possible activation of a GPCR, perhaps T2R14.

We further tested if the Ca^{2+} response was from mobilization of intracellular Ca^{2+} stores or extracellular Ca^{2+} influx from outside of the plasma membrane, GPCRs, including T2Rs, induce intracellular Ca^{2+} responses, primarily from the ER [68-71].

To elucidate whether the initial Ca^{2+} responses with lidocaine stimulation were from intracellular or extracellular sources, we recorded Fluo-4 responses in HBSS, with or without Ca^{2+} (via EGTA chelation of the Ca^{2+}). Cells stimulated with lidocaine in HBSS without Ca^{2+} had a similar Ca^{2+} peak but faster rate of returning to baseline fluorescence compared with cells stimulated in HBSS with Ca^{2+} (Fig. 3A). This shows that the initial Ca^{2+} response observed with lidocaine comes from an intracellular source as there was no significant differences between the peak Ca^{2+} with or without extracellular Ca^{2+} (Fig. 3B). However, the sustained response likely involves restorative Ca^{2+} influx, possibly via

STIM1/Orai [72, 73]. As a control, cells were also incubated to kb-r7943, a plasma membrane Na^+/Ca^{2+} exchanger inhibitor [74]. There were no significant changes in lidocaine-induced Ca^{2+} responses (Supplemental Fig 2A).

GPCR activation and elevation of intracellular Ca^{2+} can also cause influx of Ca^{2+} into the mitochondria [75, 76]. We used a mitochondrial-specific fluorescent Ca^{2+} biosensor, pcDNA-4mt3cpv, to measure mitochondrial Ca^{2+} influx [56] (Fig 3E). Upon stimulation, a significant influx of Ca^{2+} into the mitochondria was observed with lidocaine and ATP (Fig 3C & D). The influx with lidocaine stimulation was significantly greater than both equivalent and greater concentrations of denatonium benzoate (10 and 15mM). In addition, an ER-specific fluorescent Ca^{2+} biosensor, pcDNA-D1ER, was used to measure ER Ca^{2+} efflux [56] (Fig 3H). Lidocaine stimulation caused a significant decrease in ER Ca^{2+} compared to equivalent or greater concentrations of denatonium benzoate (10 and 15 mM) (Fig 3F & G). The timing of the Ca^{2+} response with lidocaine in HBSS without Ca^{2+} coincided with that of the mobilization events of the mitochondria and the ER, suggesting that the influxes/effluxes were a product of the initial intracellular response (Fig 3A, 3D & 3G).

Lidocaine activates T2R14

Following GPCR activation, GTP-bound guanine nucleotide-binding proteins (G proteins) disassociate from their receptors and carry out the effector actions [77, 78]. As GPCRs, T2Rs can couple to $G\alpha_{gustducin}$ or $G\alpha_i$, $G\beta_{1/3}$ and $G\gamma$ [20, 31, 79]. To test if lidocaine is activating a GPCR, cells were incubated with suramin, a pan-inhibitor of G protein association to their receptors. Fluo-4 Ca^{2+} responses were recorded with lidocaine stimulation with or without suramin [80]. Inhibition of G proteins with suramin significantly dampened Ca^{2+} responses with lidocaine (Fig 4A). Cells were also incubated with pertussis toxin, an inhibitor of $G\alpha_{i/o}$ subunits [81]. Upon stimulation with lidocaine, cells with pertussis toxin incubation had significantly dampened Ca^{2+} responses (Fig 4B). This is suggestive of the effects of G proteins and, therefore, GPCRs activated by lidocaine being responsible for primary Ca^{2+} responses in HNSCC cells. Interestingly, cells incubated with pertussis toxin and stimulated with denatonium benzoate had no significant differences in Ca^{2+} responses (Supplemental Fig 2B). Cells were also incubated with YM 254890, a $G\alpha q/11$ selective inhibitor [82]. While YM 25480 significantly decreased Ca^{2+} responses with T2R4 agonist denatonium benzoate, it did not affect responses with lidocaine (Supplemental Fig 2C). siRNA targeting T2R4 significantly downregulated Ca^{2+} responses with denatonium benzoate, while leaving responses with lidocaine unchanged (Supplemental Fig 2D-E). These data support previous studies that denatonium benzoate interacts with separate T2R isoforms than lidocaine [54].

GPCR activation of phospholipase C also produces diacylglycerol (DAG) [83]. To understand if lidocaine affected DAG production, an RFP DAG sensing baculovirus was

transduced into cells. Lidocaine stimulation significantly increased DAG production compared to HBSS alone (Fig 4C).

In addition, Gαi-coupling would be expected to be accompanied by a decrease in cAMP, which was measured using a fluorescent cytosolic cAMP biosensor, Flamindo2 [57]. Lidocaine significantly decreased cAMP when compared to HBSS alone (Fig 4D). Isoproterenol, a β-adrenergic agonist, was used a positive control to increase cAMP. When taking timing of these events/productions into account, the observed PTX-senstive intracellular Ca^{2+} responses coincide with both increases in DAG and decreases in cAMP, suggesting lidocaine activates a Gαi-coupled GPCR.

To understand if lidocaine interacts with T2R14 specifically, cells were incubated with 100 μM 6-methoxyflavonone (6-MF), a T2R14 antagonist [84]. Incubation with 6-MF significantly decreased Ca^{2+} responses with lidocaine stimulation (Fig 4E & F). 6-MF also significantly dampened responses with flufenamic acid and thujone, two other T2R14 agonists (Fig 4E). 6-MF did not alter Ca^{2+} responses with denatonium benzoate, a non-T2R14 agonist (Fig 4E). A recent preprint also identified several other structurally-distinct T2R14 inhibitors [58]. We purchased and tested two of these inhibitors, LF1 and LF22, and found that they both also blocked the Ca^{2+} responses to both lidocaine and flufenamic acid (Fig 4F). Taken together, these data indicate that lidocaine interacts with a GPCR in HNSCC cells, likely T2R14, to trigger an intracellular Ca^{2+} response.

Lidocaine decreases cell viability and mitochondrial membrane potential

Lidocaine is actively being investigated as a chemotherapeutic for several cancers [53, 64, 85], but its mechanism of action is completely unknown. After establishing an interaction between T2R14 and lidocaine, we tested if it had anti-proliferative effects in HNSCC cells. Using a crystal violet assay, we found that 10 mM lidocaine significantly decreased cellular proliferation after just 6 hours (Supplemental Fig 3A). After 24 hours, concentrations as low as 1 mM significantly decreased cellular proliferation (Supplemental Fig 3B).

To measure cell viability, We used an XTT assay as an indirect measurement of cellular NADH production [86]. Lidocaine (5 mM and 10 mM) and denatonium benzoate reduced cell viability in SCC 47 cells (Fig 5A). This was observed after only 2 hours, with the full assay covering 6 hours. Although we previously showed the ability of denatonium benzoate to decrease cell viability, this finding with lidocaine in HNSCC cells is novel [29, 45]. These results were also observed in both FaDu and SCC 4 cells. FaDu cells appeared to be more sensitive to denatonium benzoate than lidocaine, as 5 mM denatonium benzoate decreased cell viability, but 5 mM lidocaine did not (Fig 5B). Both 10 mM lidocaine and 10 mM denatonium benzoate decreased FaDu cell viability (Fig 5B). Conversely, only 10 mM lidocaine (not denatonium benzoate) decreased SCC 4 cell viability (Supplemental Fig 3C). These data suggest that different types of HNSCCs may have different sensitivities to specific T2R agonists.

After observing Ca^{2+} mobilization with ATP in previous experiments (Fig 1A-C), we wanted to test if this molecule would also decrease cell viability. Concentrations ranging from 1 – 100 uM ATP did not affect cell viability (Supplemental Fig 3D).

Mitochondrial membrane potential (MMP) is an indicator of overall mitochondrial health, as it affects the bulk supply of ATP production [87, 88]. A hyperpolarized MMP promotes a healthy state, while the MMP will become depolarized in response to cellular stressors [89, 90]. We used a ratiometric JC-1 assay to assess mitochondrial health in HNSCC cells in response to lidocaine. We found that 10 mM lidocaine significantly depolarized the mitochondrial membrane (Fig 5C-D). This was measured using a ratio of "green dye monomers" to "red dye aggregates", where monomers represent a depolarized mitochondrial state and aggregates represent a hyperpolarized mitochondrial state. These changes were observed as early as 100 minutes during the assay. Both decreased cell proliferation and viability, and depolarization of the mitochondrial membrane highlights the potential chemotherapeutic effects of lidocaine.

Lidocaine induces apoptosis via T2R14

After establishing the ability of lidocaine to decrease cell proliferation and viability, and to depolarize the mitochondrial membrane, we wanted to know if lidocaine could induce cell death. Lidocaine induces apoptosis in a variety of cancer and non-cancer settings [37, 52, 91-95]. While lidocaine can induce apoptosis in cancers of the esophageal and thyroid (organs that are localized near the internal regions of the head and neck), it remains unknown if the local anesthetics induce apoptosis, or even cell death, in HNSCC cells [96-98].

We utilized the CellEvent assay to measure caspase-3 and -7 cleavage in HNSCC cells with lidocaine. The green CellEvent dye fluoresces upon cleavage with either caspase-3 or -7 if/when apoptosis occurs [99-101]. This assay revealed that lidocaine induces apoptosis in SCC 47 and FaDu cells (Fig 6A & B; Supplemental Fig 4A). Interestingly, SCC 47 cells were more sensitive to lidocaine-induced apoptosis than FaDu cells, as it took FaDu cells longer to undergo caspase cleavage (Fig 6B; Supplemental Fig 4A). Differential Interference Contrast (DIC) images were taken in parallel with the CellEvent assay in SCC 47 cells. The images reveal poor cellular morphology coinciding with the apoptosis (Supplemental Fig 4B). To further verify caspase cleavage, full length and cleaved forms of both caspases were Western blotted for in SCC 47 cells using 10 mM lidocaine over 6 hours. Caspase-7 cleavage occurred as early as 2 hours, while caspase-3 cleavage occurred as early as 4 hours (Fig 6C).

To better understand if the observed apoptosis was a direct function of T2R14 activation via lidocaine, we used the CellEvent assay again, with or without 6-MF (T2R14 antagonist). When we first repeated the XTT assay in SCC 47 cells with or without 6-MF, the 6-MF did not rescue viability during co-incubation with lidocaine (Supplemental Fig 4D). However, we found that after 10 hours, 6-MF was able to block apoptosis in SCC 47

co-incubated with 10 mM lidocaine (Fig 6D & Supplemental Fig 4C). Complimentary to our original CellEvent data, DIC images revealed that 6-MF preserves overall cell morphology, even in the presence of lidocaine (Supplemental Fig 4C). We hypothesize that this is because 6-MF reduces T2R14 signaling to a level where apoptosis is blocked but proliferation is still halted. However, this shows for the first time that lidocaine can induce apoptosis in HNSCC via activation of a T2R, specifically T2R14. This is a novel mechanism that could be advantageous in treating HNSCCs or other cancers

Lidocaine may inhibit the proteasome as a mechanism of apoptosis

There are several mechanisms suggested by which lidocaine can induce apoptosis in mammalian cells [102-105]. However, similarly to studying the effects of lidocaine in HNSCCs, its mechanism(s) of inducing apoptosis following T2R14 activation is/are completely unknown. It is vital to understand how a compound induces apoptosis in order to utilize it appropriately.

When we Western blotted for caspase-3 and -7 cleavage as markers of apoptosis activation, we noticed that not only were the cleaved forms of the proteins increasing, but so were the full-length forms (Fig 6C). We wanted to know if HNSCC cells were upregulating caspase-3 and -7 production (i.e., mRNA transcription or protein translation) in response to lidocaine, or if there was inhibition of normal proteolytic degradation processes. Caspase-3 and -7 production was measured via qPCR. There were no differences between mRNA at 0- and 6-hours post-lidocaine (Fig 7A). These proteins were then blotted for +/- 10 mM lidocaine and/or cycloheximide, which blocks new translation of proteins in cells [106]. Even with this blockade, 10 mM lidocaine still showed upregulation of full-length caspase-3 and -7 proteins (Fig 7B & C). This indicates that lidocaine may inhibit normal protein degradation pathways as a mechanism of inducing apoptosis.

In order to investigate the clinical applications of lidocaine, a gel was formulated using Matrigel to model the actual vehicle in which the lidocaine would be applied. Using both “thin” and “thick” formulations, we found that lidocaine induced cell death over 24 hours when compared to control via DIC images. The thick formulation appeared to have the most death, as compared to the thin formulation (Fig 8).

Discussion

With only 50% of patients surviving past five years even with treatment, the outlook for HNSCC patients is bleak [10, 107]. Standard treatment options (surgery, radiotherapy, chemotherapy) leave lasting effects [108-111]. Cetuximab, an EGFR inhibitor, is considered to be the only “targeted” chemotherapy approved by the FDA to treat HNSCCs [14]. Still, this chemotherapy does not distinguish between cancerous and non-cancerous cells [112]. In addition, immunotherapies are actively being investigated for HNSCCs; however, there are none that have been approved by the FDA [6, 113]. Novel, and

possible targeted, therapies must be discovered to improve outcomes for HNSCC patients.

Data here suggest that T2Rs may be an attractive target to leverage against HNSCCs using existing clinical compounds. T2R expression is not limited to just the oral cavity but also in all epithelial regions affected by HNSCCs [114]. Although T2Rs are low affinity-GPCRs, their agonists have detrimental effects on HNSCC cell health, mitochondrial membrane potential, and cell survival [45]. An advantage of HNSCC is that lidocaine could be implemented into the clinic as a topical chemotherapeutic (e.g., an eluting gel or topical rinse). This is due to the accessibility of the internal regions of the head. Essentially, this treatment would be localized to the interest of region, hopefully leaving surrounding normal tissue unaffected [115]. Lidocaine already comes in a topical/cream form, and topical chemotherapies are being investigated as new routes of treatment [116-118]. In some cases of oral and oropharynx SCC, we found that T2R14 expression is upregulated, indicating the potential of developing targeted therapies, on a case-by-case basis for this receptor [45]. As a local anesthetic that also activates T2R14, the potential effects of lidocaine as a chemotherapeutic bitter agonist for HNSCCs has not been explored [54]. With high solubility, documented safety data, and the use of it in the HNSCC surgery setting, lidocaine has the potential to be an easily translatable treatment for these cancers [119, 120].

Here, we established interactions between lidocaine and T2R14 first via Ca^{2+} responses in HNSCC immortalized cells lines. Compared to other T2R agonists including flufenamic acid, thujone, and denatonium benzoate (the most bitter compound currently known in terms of taste perception), lidocaine stimulation produced the largest Ca^{2+} responses. However, agonists could only be compared at their maximum aqueous solubility. Flufenamic acid is not nearly as soluble as the aforementioned compounds, which prevented us from using mM concentrations. While denatonium benzoate and thujone shared similar concentrations as lidocaine in the millimolar range, flufenamic acid did not, making this an inaccurate comparison of potency. However, this is indicative that lidocaine may be more easily translatable into the clinic due to high solubility. Procaine which has a bitter taste, but no identified T2R interaction, had minimal effects on Ca^{2+} , suggesting the effects of lidocaine are not due to Na^{+} channel inhibition. In addition, ATP produced significant Ca^{2+} responses in HNSCC cells at only 100 uM yet did not have any effects on cell viability like bitter agonists (Fig 1A-C; Supplemental Fig 3E) [62].

Both suramin and pertussis toxin dampened lidocaine Ca^{2+} responses (Fig. 4A & B) [80, 81]. This further links the Ca^{2+} response induced by lidocaine and generalized GPCR activation. However, suramin and pertussis toxin did not fully abolish the Ca^{2+} response with lidocaine. Lidocaine can also activate TRPVA1 and TRPV1 Ca^{2+} influx in neuronal cells [121]. TRP channels might be expressed in HNSCC cells [122-124]. There may be some TRP channel activity causing the small Ca^{2+} responses with the G protein inhibitors. Additionally, TRP channels could play roles in the sustained Ca^{2+} response

observed with lidocaine. Incubation with pertussis toxin did not affect Ca^{2+} response with denatonium benzoate, suggesting that the compound interacts with different T2Rs that are differently coupled (Supplemental Fig 2A) [125, 126]. Ca^{2+} responses with denatonium benzoate, but not lidocaine were dampened with YM-254890, a $G\alpha_q$ inhibitor, and with siRNA knockdown of T2R4 (Supplemental Fig 2A & C-E) [127]. Although T2Rs are primarily coupled to $G\alpha_{gustducin}$ or $G\alpha_l$, there is also evidence that they may be coupled to $G\alpha_{q14}$ as well [128]. This could explain the dampened Ca^{2+} response with YM-254890.

Lidocaine also caused a decrease in cAMP and an increase in DAG, indicative of GPCR activation, likely coupled to pertussis toxin-sensitive $G\alpha_{gustducin}$ or $G\alpha_i$ [29, 129]. We found that 6-MF, a specific T2R14 antagonist, also dampened Ca^{2+} responses with lidocaine and other T2R14 agonists, suggesting activation of T2R14 [130]. Similar to suramin and pertussis toxin, the Ca^{2+} responses with 6-MF were not completely blocked, possibly due to incomplete antagonism or cross-reactivity with another T2R.

Some studies have investigated whether lidocaine can be repurposed as a chemotherapeutic in several cancers [48, 52, 131, 132]. This is a promising and low-cost endeavor as the local anesthetic is already used in surgical resection for many cancers and is FDA approved [133]. However, none of these studies have focused on HNSCCs, and none have considered activation of T2R14 [97, 134]. Here, we found that lidocaine alone significantly decreased HNSCC cell viability (measured via NADH production) and depolarized the mitochondrial membrane, which is indicative of poor mitochondrial health. Lidocaine decreased cell proliferation at just 6 hours. Mitochondria are a primary source of NADH production, showing the parallel of both observed cell viability (which measures NADH production) and observed mitochondrial membrane depolarization. Interestingly, 6-MF did not rescue cell viability with lidocaine. Whether this is indicative of mechanisms of decreased cell viability in response to lidocaine being independent from T2R14 activation and/or Ca^{2+} mobilization or simply incomplete antagonism of the receptor remains to be determined. 6-MF did block the apoptosis induced by lidocaine, as measured by caspase-3 and -7 cleavage with fluorescent dye [101, 135, 136].

Our data also suggest lidocaine inhibits proteasomal degradation of several proteins, including caspases and cyclin D [137, 138]. The ubiquitin-proteasome system (UPS) is a complex made up of many subunits that have protease activity. This complex can capture poly-ubiquinated proteins, unfold them, and subject them to proteolysis [139]. Whether or not lidocaine initiates this inhibition of the proteasome through activation of T2R14, or another independent mechanism, will be tested in future studies. Intracellular Ca^{2+} mobilization is essential for proper proteasome activity in neuronal models, mainly through the activation of calcium/calmodulin-dependent protein kinase II (CaMKII) [140-142]. In addition, the UPS is also responsible for regulating intracellular Ca^{2+} via degradation of Ca^{2+} channels and pores [143]. A link between T2R14-induced Ca^{2+} mobilization and inhibition of the UPS remains to be determined.

Another primary mechanism of UPS regulation is through the mitochondria. Mitochondria can negatively regulate proteasomal activity via increased ROS and decreased ATP [144-146], which can be a result of mitochondrial membrane depolarization, as observed here with lidocaine stimulation [147]. It is also possible that, independent of T2R14 activation, lidocaine is able to diffuse into the cell [148]. Lidocaine may inhibit the UPS by binding to the β5 subunit of the 20s proteasome in p53-postive cancer cells [149]. In any case, UPS inhibition can be linked to apoptosis [150-153]. Drugs that inhibit the catalytic activity of the UPS, including hallmark drugs like bortezomib and ixazomib [154] are used as chemotherapeutics as cancer cells have high rates of protein-turnover for survival [155]. This may contribute to apoptosis observed with lidocaine stimulation, either downstream of T2R14 activation or independently.

It is highly important to continue to study and uncover new therapeutics and therapeutic targets to better outcomes for HSNCC patients. Our data suggest using lidocaine to treat HNSCCs could prove to be a promising strategy, warranting further in vivo and clinical investigation. Due to accessibility of the internal regions of the head and neck, lidocaine could be delivered as a topical cream or local injection. This would enable the use of potent doses without affecting other regions of the body. We observed here that lidocaine in the form of gel inhibited proliferation in HNSCC cells. This strategy could be used post-surgery to kill residual cancer cells, perhaps decreasing the amount of tissue needed to be resected and chance of metastasis.

Acknowledgements

We thank M. Victoria (University of Pennsylvania) for excellent technical assistance. This study was supported by T32GM008076 (Z.A.M.), an American Head and Neck Society Pilot Grant (R.M.C.), R01DC016309 (R.J.L.)

CRediT authorship contribution statement:

Zoey A. Miller: Conceptualization, Investigation, Methodology, Formal analysis, Writing – original draft, Writing – review & editing; Jennifer F. Jolivert: Investigation; Sahil Muthuswami: Investigation; Arielle Mueller: Investigation; Derek B. McMahon: Conceptualization, Methodology; Ryan M. Carey: Resources, Conceptualization, Funding acquisition; Robert J. Lee: Conceptualization, Writing – review & editing, Project administration, Supervision, Funding acquisition.

Figures

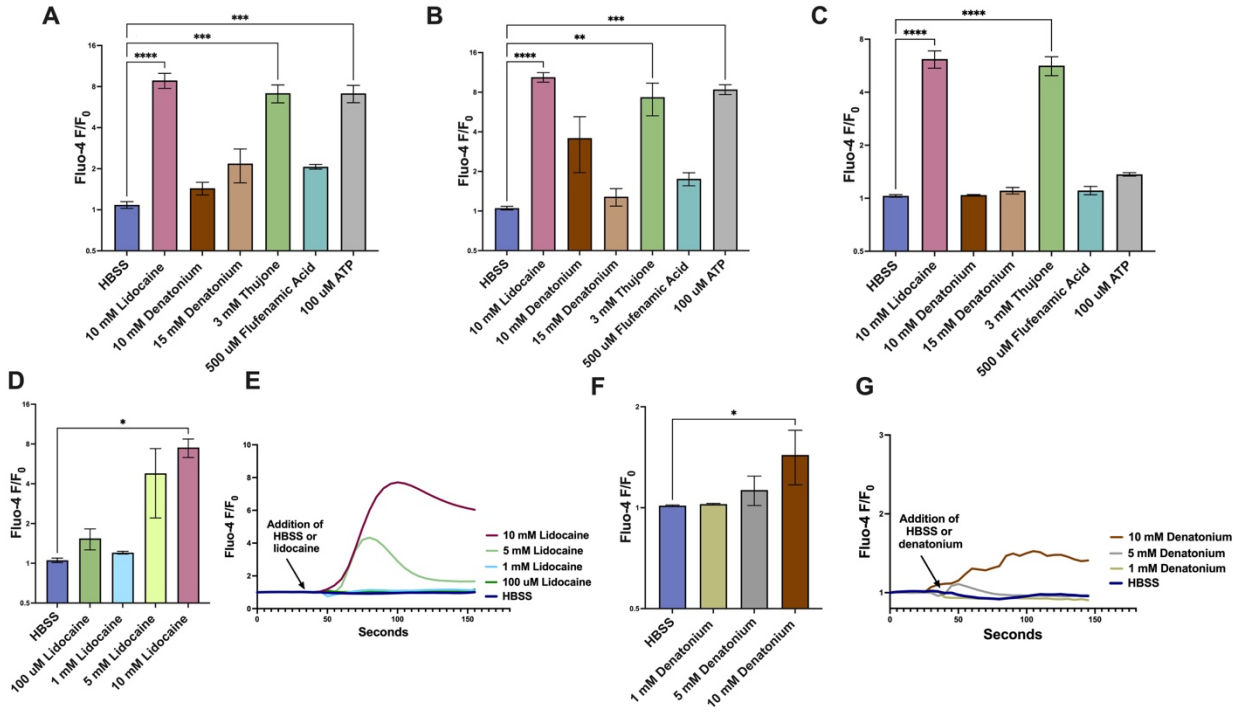

Figure 1. Lidocaine induced Ca^{2+} responses in HNSCC cells. HNSSC cell lines SCC 47, FaDu, and RPMI 2650, were loaded with Fluo-4 and imaged for subsequent Ca^{2+} responses with bitter agonists. **A)** SCC 47 peak fluorescent Ca^{2+} responses with HBSS, 10 mM lidocaine, 10 mM denatonium benzoate, 15 mM denatonium benzoate, 3 mM thujone, 500 μM flufenamic acid, or 100 μM ATP. **B)** FaDu peak fluorescent Ca^{2+} responses with HBSS, 10 mM lidocaine, 10 mM denatonium benzoate, 15 mM denatonium benzoate, 3 mM thujone, 500 μM flufenamic acid, or 100 μM ATP. **C)** RPMI 2650 peak fluorescent Ca^{2+} responses with HBSS, 10 mM lidocaine, 10 mM denatonium benzoate, 15 mM denatonium benzoate, 3 mM thujone, 500 μM flufenamic acid, or 100 μM ATP. **D)** SCC 47 peak fluorescent Ca^{2+} responses with 0 – 10 mM lidocaine. **E)** SCC 47 representative fluorescent Ca^{2+} responses from one experiment over time with 0 – 10 mM lidocaine. **F)** SCC 47 peak fluorescent Ca^{2+} responses with 0 – 10 mM denatonium benzoate. **G)** SCC 47 representative fluorescent Ca^{2+} responses from one experiment over time with denatonium benzoate. Peak fluorescence mean +/- SEM with >3 experiments using separate cultures. Significance by 1-way ANOVA with Bonferroni posttest comparing HBSS to each agonist. $P < 0.05$ (*), $P < 0.01$ (**), $P < 0.001$ (***), and no statistical significance (ns).

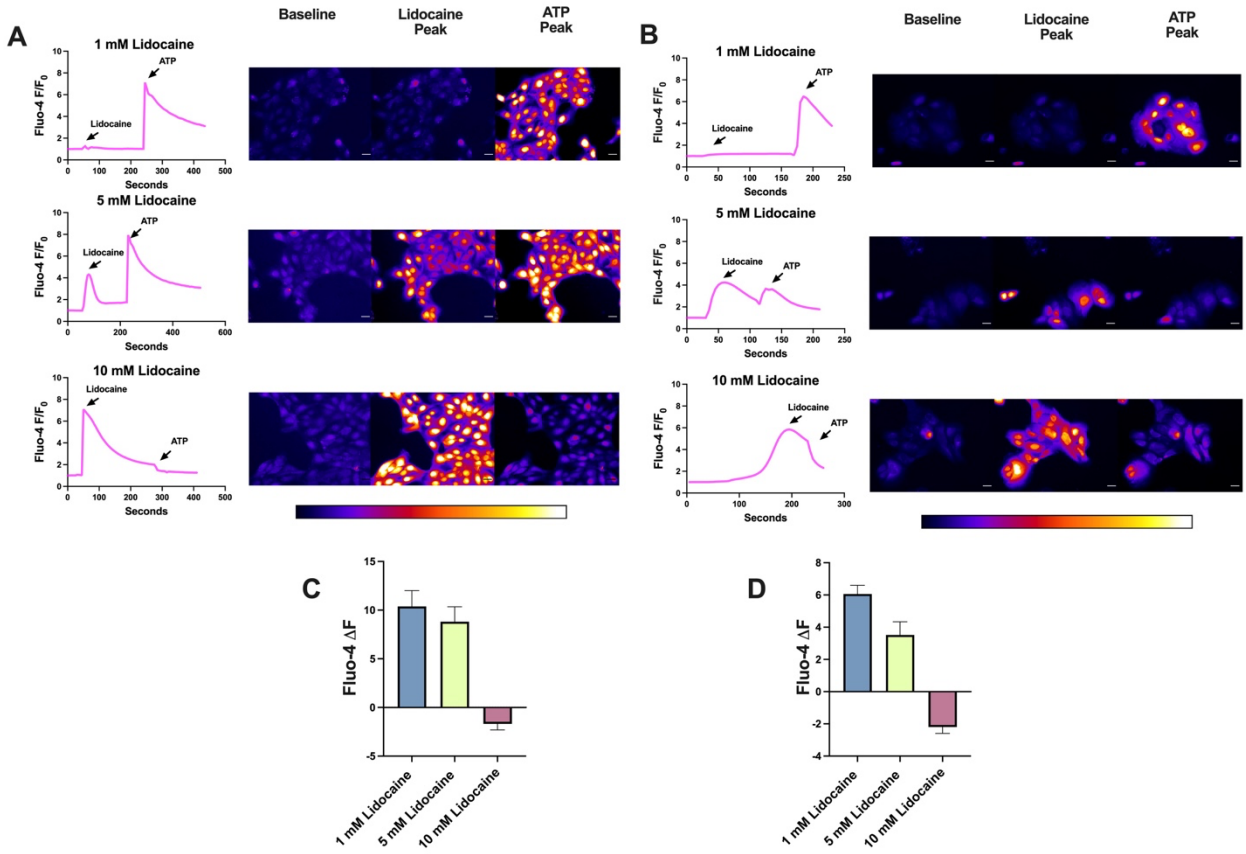

Figure 2. Lidocaine exhausts purinergic Ca^{2+} responses in HNSCC cells. SCC 47 and SCC 4 cells were loaded with Fluo-4 and imaged for subsequent Ca^{2+} responses with 1 – 10 mM lidocaine followed by 100 μM ATP. **A)** SCC 47 fluorescent Ca^{2+} responses over time and representative images of responses of baseline, lidocaine peak and ATP peak with 1 – 10 mM lidocaine followed by 100 μM ATP. Scale bars = 30 μm. **B)** SCC 4 fluorescent Ca^{2+} responses over time and representative images of responses of baseline, lidocaine peak and ATP peak with 1 – 10 mM lidocaine followed by 100 μM ATP. Scale bars = 30 μm. **C)** SCC 47 change in fluorescence with secondary ATP simulation. **D)** SCC 4 change in fluorescence with secondary ATP simulation.

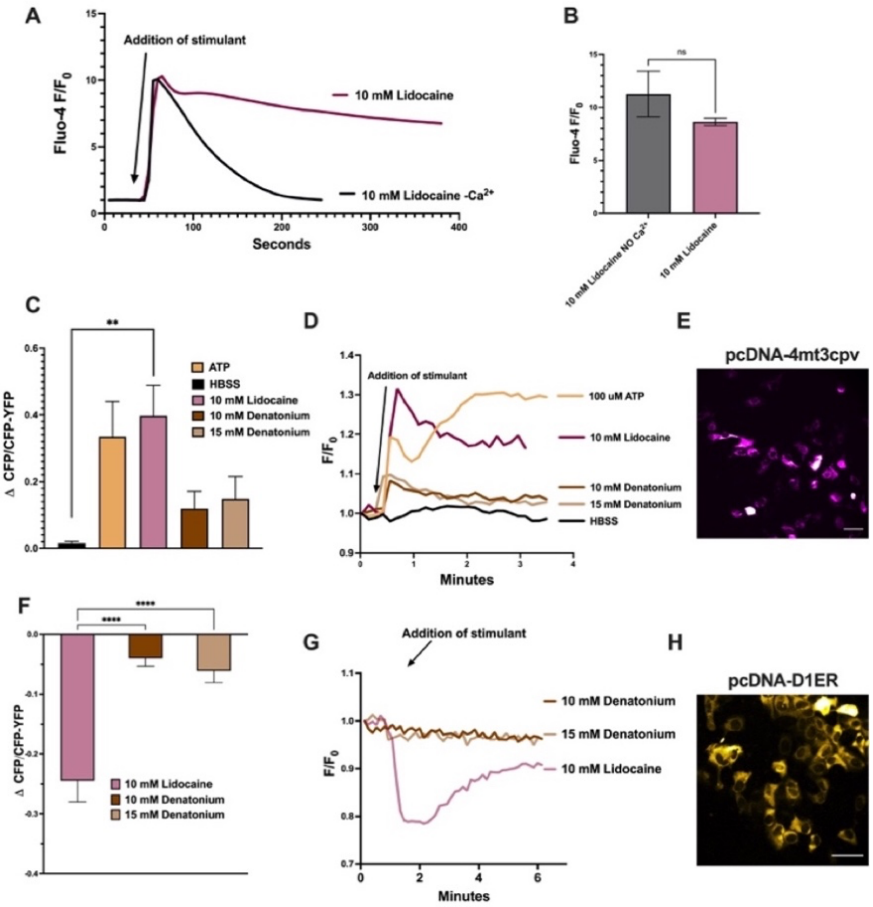

Figure 3. Ca^{2+} response with lidocaine is due to intracellular Ca^{2+} release. HNSSC cell line, SCC 47, was loaded with 5 μM Fluo-4-AM fluorescent Ca^{2+} dye indicator for 50 min and imaged for subsequent Ca^{2+} responses with 10 mM lidocaine. **A)** SCC 47 fluorescent Ca^{2+} response over time in HBSS with or without Ca^{2+} (+/- extracellular Ca^{2+}). **B)** SCC 47 peak fluorescent Ca^{2+} responses with 10 mM lidocaine in HBSS with or without Ca^{2+}. Peak fluorescent mean +/- SEM with >3 separate cultures. Significance by unpaired t-test. SCC 47 cells were transfected with pcDNA-4mt3cpv or pcDNA-D1ER 24 – 48 hours prior to Ca^{2+} imaging. **C)** SCC 47 mitochondrial peak CFP/CFP-YFP fluorescent Ca^{2+} responses with HBSS, ATP, 10 mM lidocaine, 10 mM denatonium benzoate, or 15 mM denatonium benzoate. Peak fluorescence mean +/- SEM with >3 experiments using separate cultures. Significance by 1-way ANOVA with Bonferroni posttest comparing HBSS to each agonist. **D)** SCC 47 mitochondrial fluorescent Ca^{2+} responses over time with HBSS, ATP, 10 mM lidocaine, 10 mM denatonium, or 15 mM denatonium. **E)** SCC 47 representative image of pcDNA-4mt3cpv CFP/YFP baseline fluorescence mitochondrial localization. Scale bar = 30 μm. **F)** SCC 47 ER peak CFP/CFP-YFP fluorescent Ca^{2+} responses with10 mM lidocaine, 10 mM denatonium benzoate, or 15 mM denatonium benzoate. Peak fluorescence mean +/- SEM with >3 experiments using separate cultures. Significance by 1-way ANOVA with Bonferroni posttest comparing HBSS to each agonist. **G)** SCC 47 ER fluorescent Ca^{2+} responses over time with 10 mM lidocaine, 10 mM denatonium benzoate, or 15 mM denatonium benzoate. **H)** SCC 47 representative image of pcDNA-D1ER CFP/YFP baseline fluorescence ER localization. Scale bar = 30 μm. $P < 0.05$ (*), $P < 0.01$ (**), $P < 0.001$ (***), and no statistical significance (ns or no indication).

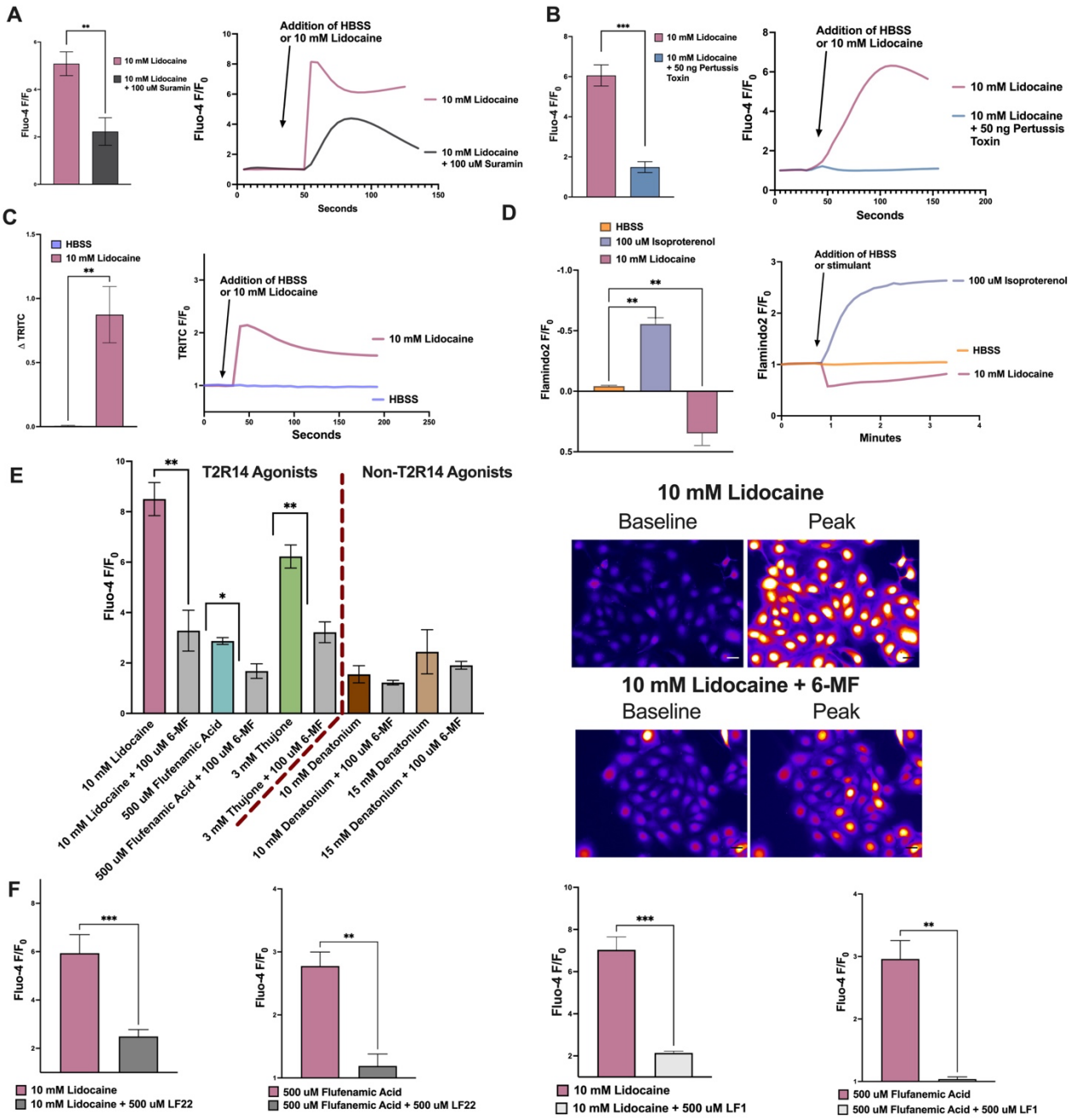

Figure 4. Lidocaine increases intracellular Ca^{2+} through activation of T2R14. HNSSC cell line, SCC 47, was loaded with Fluo-4 and imaged for subsequent Ca^{2+} responses with 10 mM lidocaine. **A)** SCC 47 peak fluorescent Ca^{2+} and accompanying representative Ca^{2+} traces over time of 10 mM lidocaine with or without 1 hour prior incubation with 100 μM suramin. **B)** SCC 47 peak fluorescent Ca^{2+} and accompanying representative Ca^{2+} traces over time of 10 mM lidocaine with or without 18 hour prior incubation with 50 ng pertussis toxin. Peak fluorescent mean +/- SEM with >3 separate cultures. Significance by unpaired t-test. SCC 47 cells were transduced with fluorescent DAG biosensor and imaged for subsequent DAG responses with 10 mM lidocaine. **C)** SCC 47 peak fluorescent DAG and representative DAG trace over time with HBSS or 10 mM lidocaine. Peak fluorescent mean +/- SEM with >3 separate cultures. Significance by

unpaired t-test. SCC 47 cells were transfected with pcDNA3.1(-)Flamindo2 and imaged for subsequent cAMP responses with HBSS, 10 mM lidocaine or 100 μM isoproterenol. **D)** SCC 47 peak fluorescent cAMP and representative cAMP traces over time with HBSS, 100 μM isoproterenol, or 10 mM lidocaine. Peak fluorescence mean +/- SEM with >3 experiments using separate cultures. Significance by 1-way ANOVA with Bonferroni posttest comparing HBSS to each agonist. **E)** SCC 47 peak Ca^{2+} fluorescent responses and representative fluorescent images with 10 mM lidocaine with or without prior 1 hour incubation with 100 μM 6-methoxflavanone (6-MF). Peak fluorescent mean +/- SEM with >3 separate cultures. Significance by unpaired t-test between HBSS and bitter agonist response with 100 μM 6-MF. Image scale bars = 30 μm. **F)** SCC 47 peak Ca^{2+} fluorescent responses with 10 mM lidocaine with or without prior 1 hour incubation with two other structurally different T2R14 antagonists, LF1 and LF22, at 500 uM. $P < 0.05$ (*), $P < 0.01$ (**), $P < 0.001$ (***), and no statistical significance (ns or no indication).

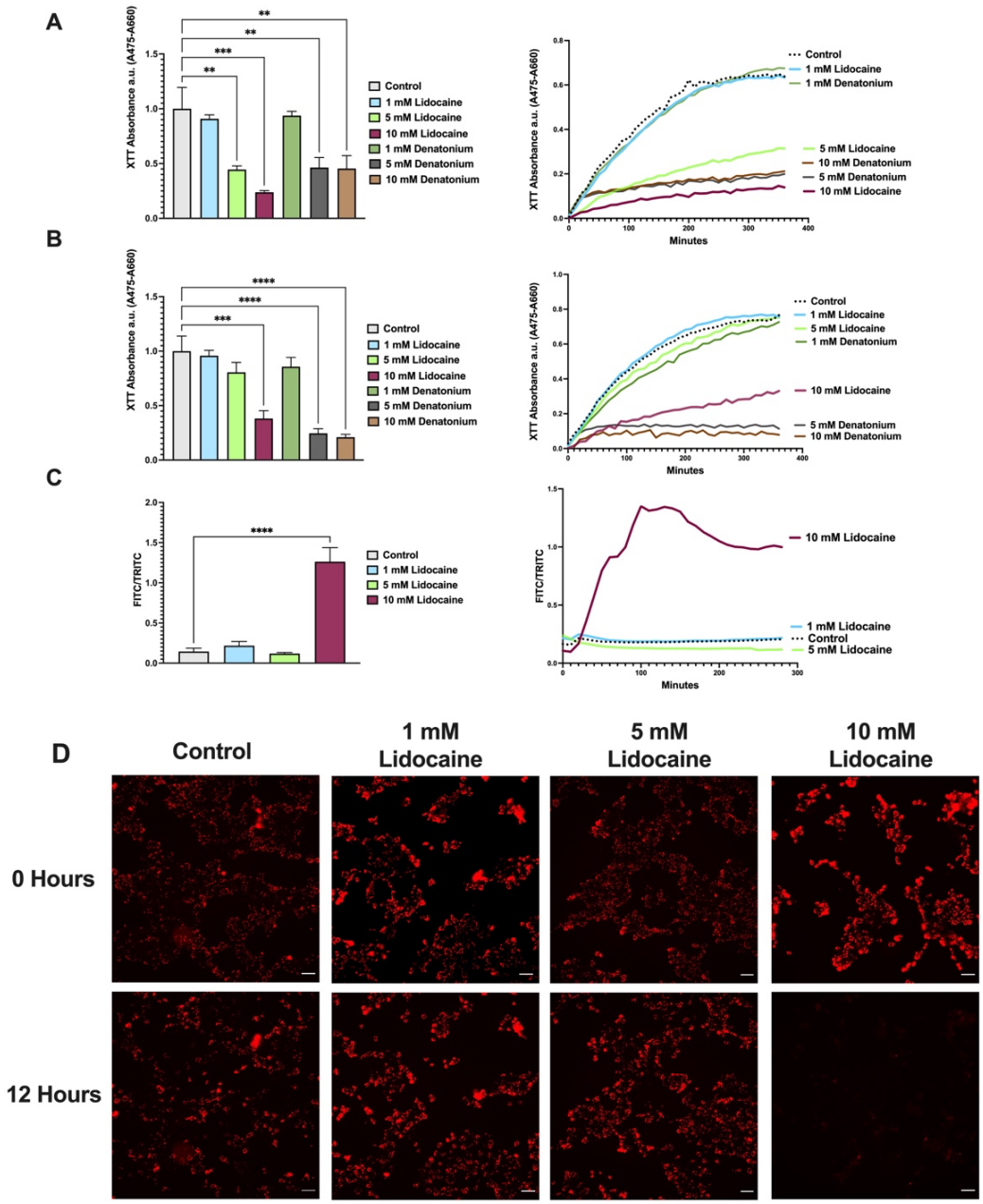

Figure 5. Lidocaine decreases cell viability and depolarizes the mitochondrial membrane. SCC 47 and FaDu cells were incubated with bitter agonists with XTT dye, an indicator of NADH production. A decrease in the difference of absorbance (475 nm – 660 nm) indicates reduced NADH production. **A)** SCC 47 XTT absorbance values (475 nm – 660 nm) after 120 minutes of incubation with media, 1 – 10 mM lidocaine, or 1 -10 denatonium benzoate. Absorbance values were measured over six hours as seen in representative traces. **B)** FaDu XTT absorbance values (475 nm – 660 nm) after 120 minutes of incubation with media, 1 – 10 mM lidocaine, or 1 -10 denatonium benzoate. Absorbance values were measured over six hours as seen in representative traces. Absorbance mean +/- SEM with >3 separate cultures. Significance by 1-way ANOVA

with Bonferroni posttest comparing media to each concentration of lidocaine and denatonium benzoate. SCC 47 cells were loaded with fluorescent JC-1 dye 15 minutes prior to incubation with bitter agonists. An increase in FITC (dye monomers) / TRTIC (dye aggregates) represents depolarized mitochondrial membrane potential. **C)** FaDu fluorescent FITC/TRITC ratio at 100 minutes of incubation with 0 – 10 mM lidocaine and representative fluorescent values over 300 minutes. Fluorescent mean +/- SEM with >3 separate cultures. Significance by 1-way ANOVA with Bonferroni posttest comparing media to each concentration of lidocaine. D) FaDu representative images of change in TRITC red dye aggregates (indicative of loss of mitochondrial membrane potential) at 0 and 12 hours with 0 – 10 mM lidocaine. Scale bars = 30 μm. $P < 0.05$ (*), $P < 0.01$ (**), $P < 0.001$ (***), and no statistical significance (ns or no indication).

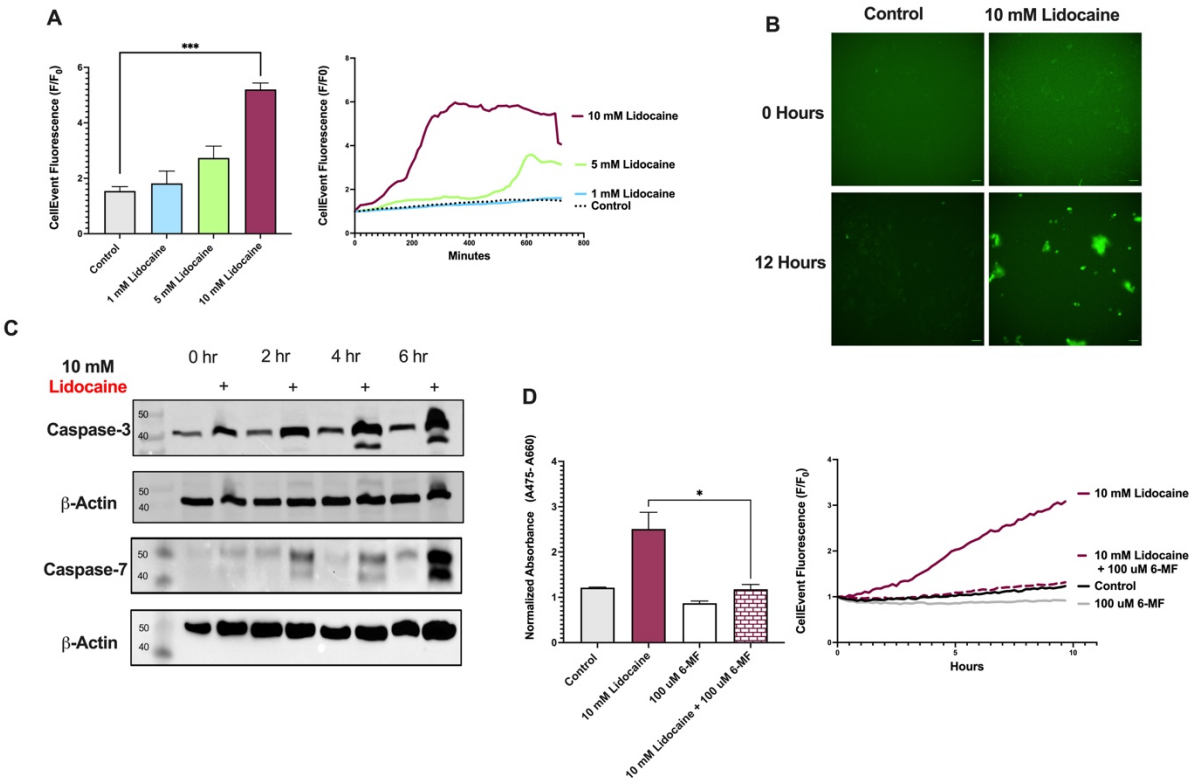

Figure 6. Lidocaine induces apoptosis via T2R14. SCC 47 cells were incubated with 10 mM lidocaine with CellEvent fluorescent dye, which fluoresces upon caspase-3 and caspase-7 cleavage. A) SCC 47 CellEvent fluorescence at 4 hours with 0 - 10 mM lidocaine. Representative trace of CellEvent fluorescence over 12 hours with 10 mM lidocaine. Fluorescent mean +/- SEM with >3 separate cultures. Significance determined by one-way ANOVA with Bonferroni posttest between untreated and treated cells. B) SCC 47 representative images of CellEvent caspase cleavage at 0 and 12 hours with 10 mM lidocaine. C) SCC 47 cells were treated with 10 mM lidocaine for 0, 2, 4, or 6 hours. Caspase-3, caspase-7, and β-Actin primary antibody (1:1000) incubation in Tris-Tween with 5% BSA was 1 hour at room temperature. Incubation with goat anti-rabbit or anti-mouse IgG-horseradish peroxidase secondary antibodies (1:1000) was 1 hour at room temperature. Immunoblots shown are representative of 3 independent experiments using cells at different passage number on different days.
D) SCC 47 CellEvent fluorescence at 10 hours with 10 mM lidocaine with or without 100 μM 6-MF. Representative trace of CellEvent fluorescence over 10 hours with 10 mM lidocaine with or without 100 μM 6-MF. Mean +/- SEM with >3 separate cultures. Significance was determined by unpaired *t*-test with control between 10 mM lidocaine and 10 mM lidocaine + 100 μM 6-MF. $P < 0.05$ (*), $P < 0.01$ (**), $P < 0.001$ (***), and no statistical significance (ns or no indication).

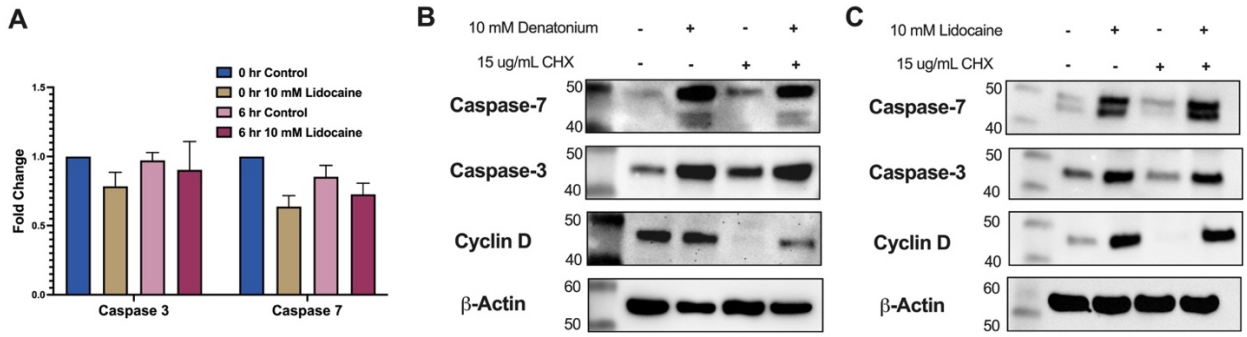

Figure 7. Lidocaine may inhibit the proteasome. SCC 47 cells were incubated with 10 mM lidocaine for 6 hours. A) SCC 47 caspase-3 and caspase-7 mRNA expression at 0 and 6 hours with or without 10 mM lidocaine. Expression is relative to 0 hour Control. Mean +/- SEM with >3 separate cultures. Significance determined by paired t-test between lidocaine treated cells at 0 and 6 hours. SCC 47 cells were treated with 10 mM denatonium benzoate or 10 mM lidocaine for 6 hours with or without 15 ug/mL cycloheximide (CHX). Caspase-3, caspase-7, cyclin D (cycloheximide protein synthesis control) and β-Actin primary antibody (1:1000) incubation in Tris-Tween with 5% BSA was 1 hour at room temperature. Incubation with goat anti-rabbit or anti-mouse IgG-horseradish peroxidase secondary antibodies (1:1000) was 1 hour at room temperature. Immunoblots shown are representative of 3 independent experiments using cells at different passage number on different days. $P < 0.05$ (*), $P < 0.01$ (**), $P < 0.001$ (***), and no statistical significance (ns or no indication).

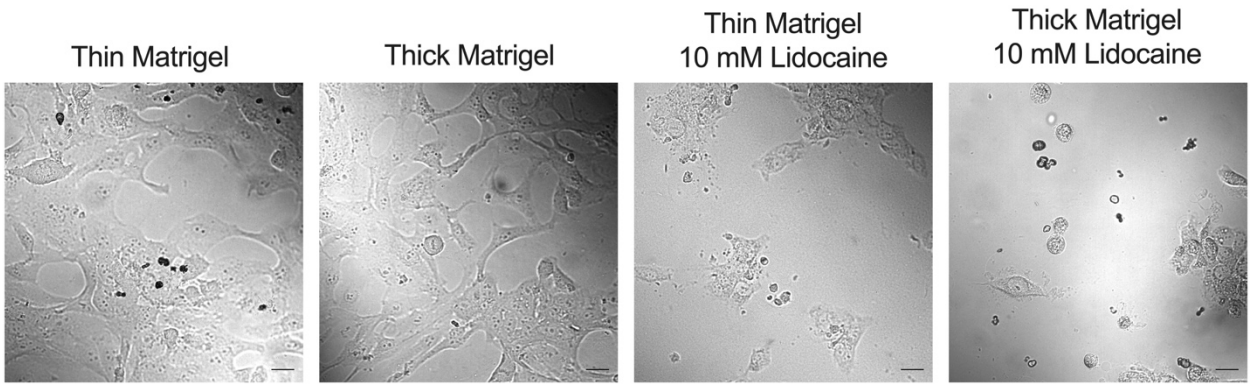

Figure 8. Translation of lidocaine into the clinic. SCC 47 cells were subjected to Matrigel containing 10 mM lidocaine for 24 hours. DIC images of SCC 47 cells after 24 hours of lidocaine-Matrigel exposure with both thick and thin formulations. Scale bars = 30 μm.

References

1. Johnson, D.E., et al., *Head and neck squamous cell carcinoma.* Nat Rev Dis Primers, 2020. **6**(1): p. 92.
2. Solomon, B., R.J. Young, and D. Rischin, *Head and neck squamous cell carcinoma: Genomics and emerging biomarkers for immunomodulatory cancer treatments.* Semin Cancer Biol, 2018. **52**(Pt 2): p. 228-240.
3. Jethwa, A.R. and S.S. Khariwala, *Tobacco-related carcinogenesis in head and neck cancer.* Cancer Metastasis Rev, 2017. **36**(3): p. 411-423.
4. Kawakita, D. and K. Matsuo, *Alcohol and head and neck cancer.* Cancer Metastasis Rev, 2017. **36**(3): p. 425-434.
5. Kamangar, F., G.M. Dores, and W.F. Anderson, *Patterns of cancer incidence, mortality, and prevalence across five continents: defining priorities to reduce cancer disparities in different geographic regions of the world.* J Clin Oncol, 2006. **24**(14): p. 2137-50.
6. Miyauchi, S., et al., *Immune Modulation of Head and Neck Squamous Cell Carcinoma and the Tumor Microenvironment by Conventional Therapeutics.* Clin Cancer Res, 2019. **25**(14): p. 4211-4223.
7. Matsuura, D., et al., *Risk factors for salvage surgery failure in oral cavity squamous cell carcinoma.* Laryngoscope, 2018. **128**(5): p. 1113-1119.
8. Hannen, E.J. and D. Riediger, *The quantification of angiogenesis in relation to metastasis in oral cancer: a review.* Int J Oral Maxillofac Surg, 2004. **33**(1): p. 2-7.
9. Irani, S., *Distant metastasis from oral cancer: A review and molecular biologic aspects.* J Int Soc Prev Community Dent, 2016. **6**(4): p. 265-71.
10. Hashim, D., et al., *Head and neck cancer prevention: from primary prevention to impact of clinicians on reducing burden.* Ann Oncol, 2019. **30**(5): p. 744-756.
11. Suh, Y., et al., *Clinical update on cancer: molecular oncology of head and neck cancer.* Cell Death Dis, 2014. **5**: p. e1018.
12. Murphy, B.A., et al., *Quality of life research in head and neck cancer: a review of the current state of the science.* Crit Rev Oncol Hematol, 2007. **62**(3): p. 251-67.
13. Rajendra, A., et al., *Palliative chemotherapy in head and neck cancer: balancing between beneficial and adverse effects.* Expert Rev Anticancer Ther, 2020. **20**(1): p. 17-29.
14. Muraro, E., et al., *Cetuximab in locally advanced head and neck squamous cell carcinoma: Biological mechanisms involved in efficacy, toxicity and resistance.* Crit Rev Oncol Hematol, 2021. **164**: p. 103424.
15. Choi, S. and J.N. Myers, *Molecular pathogenesis of oral squamous cell carcinoma: implications for therapy.* J Dent Res, 2008. **87**(1): p. 14-32.
16. Barragan, R., et al., *Bitter, Sweet, Salty, Sour and Umami Taste Perception Decreases with Age: Sex-Specific Analysis, Modulation by Genetic Variants and Taste-Preference Associations in 18 to 80 Year-Old Subjects.* Nutrients, 2018. **10**(10).
17. Zhang, J., et al., *Sour Sensing from the Tongue to the Brain.* Cell, 2019. **179**(2): p. 392-402 e15.
18. Liman, E.R., *Salty Taste: From Transduction to Transmitter Release, Hold the Calcium.* Neuron, 2020. **106**(5): p. 709-711.
19. DeSimone, J.A. and V. Lyall, *Taste receptors in the gastrointestinal tract III. Salty and sour taste: sensing of sodium and protons by the tongue.* Am J Physiol Gastrointest Liver Physiol, 2006. **291**(6): p. G1005-10.
20. Ahmad, R. and J.E. Dalziel, *G Protein-Coupled Receptors in Taste Physiology and Pharmacology.* Front Pharmacol, 2020. **11**: p. 587664.
21. Kinnamon, S.C., *Taste receptor signalling - from tongues to lungs.* Acta Physiol (Oxf), 2012. **204**(2): p. 158-68.

22. Niki, M., et al., *Gustatory signaling in the periphery: detection, transmission, and modulation of taste information.* Biol Pharm Bull, 2010. **33**(11): p. 1772-7.
23. Romanov, R.A., et al., *Afferent neurotransmission mediated by hemichannels in mammalian taste cells.* EMBO J, 2007. **26**(3): p. 657-67.
24. Bachmanov, A.A., et al., *Genetics of taste receptors.* Curr Pharm Des, 2014. **20**(16): p. 2669-83.
25. Carey, R.M. and R.J. Lee, *Taste Receptors in Upper Airway Innate Immunity.* Nutrients, 2019. **11**(9).
26. Wooding, S.P., V.A. Ramirez, and M. Behrens, *Bitter taste receptors: Genes, evolution and health.* Evol Med Public Health, 2021. **9**(1): p. 431-447.
27. Freund, J.R., et al., *Activation of airway epithelial bitter taste receptors by Pseudomonas aeruginosa quinolones modulates calcium, cyclic-AMP, and nitric oxide signaling.* J Biol Chem, 2018. **293**(25): p. 9824-9840.
28. Freund, J.R. and R.J. Lee, *Taste receptors in the upper airway.* World J Otorhinolaryngol Head Neck Surg, 2018. **4**(1): p. 67-76.
29. McMahon, D.B., et al., *The bitter end: T2R bitter receptor agonists elevate nuclear calcium and induce apoptosis in non-ciliated airway epithelial cells.* Cell Calcium, 2022. **101**: p. 102499.
30. Wu, S.V., et al., *Expression of bitter taste receptors of the T2R family in the gastrointestinal tract and enteroendocrine STC-1 cells.* Proc Natl Acad Sci U S A, 2002. **99**(4): p. 2392-7.
31. Pydi, S.P., R.P. Bhullar, and P. Chelikani, *Constitutive activity of bitter taste receptors (T2Rs).* Adv Pharmacol, 2014. **70**: p. 303-26.
32. Goricanec, D., et al., *Conformational dynamics of a G-protein alpha subunit is tightly regulated by nucleotide binding.* Proc Natl Acad Sci U S A, 2016. **113**(26): p. E3629-38.
33. Sriram, K. and P.A. Insel, *G Protein-Coupled Receptors as Targets for Approved Drugs: How Many Targets and How Many Drugs?* Mol Pharmacol, 2018. **93**(4): p. 251-258.
34. Khan, A.S., A. Hichami, and N.A. Khan, *Taste perception and its effects on oral nutritional supplements in younger life phases.* Curr Opin Clin Nutr Metab Care, 2018. **21**(5): p. 411-415.
35. Vesnina, A., et al., *Genes and Eating Preferences, Their Roles in Personalized Nutrition.* Genes (Basel), 2020. **11**(4).
36. Jeruzal-Swiatecka, J., W. Fendler, and W. Pietruszewska, *Clinical Role of Extraoral Bitter Taste Receptors.* Int J Mol Sci, 2020. **21**(14).
37. LaBonte, M.L. and M.A. Beers, *An alternative laboratory designed to address ethical concerns associated with traditional TAS2R38 student genotyping.* Biochem Mol Biol Educ, 2015. **43**(2): p. 100-9.
38. Lee, R.J., et al., *T2R38 taste receptor polymorphisms underlie susceptibility to upper respiratory infection.* J Clin Invest, 2012. **122**(11): p. 4145-59.
39. Lee, R.J., et al., *Mouse nasal epithelial innate immune responses to Pseudomonas aeruginosa quorum-sensing molecules require taste signaling components.* Innate Immun, 2014. **20**(6): p. 606-17.
40. Bloxham, C.J., S.R. Foster, and W.G. Thomas, *A Bitter Taste in Your Heart.* Front Physiol, 2020. **11**: p. 431.
41. Clark, A.A., et al., *TAS2R bitter taste receptors regulate thyroid function.* FASEB J, 2015. **29**(1): p. 164-72.
42. Zehentner, S., et al., *The Role of Bitter Taste Receptors in Cancer: A Systematic Review.* Cancers (Basel), 2021. **13**(23).
43. Martin, L.T.P., et al., *Bitter taste receptors are expressed in human epithelial ovarian and prostate cancers cells and noscapine stimulation impacts cell survival.* Mol Cell Biochem, 2019. **454**(1-2): p. 203-214.

44. Singh, N., et al., *Chemosensory bitter taste receptors T2R4 and T2R14 activation attenuates proliferation and migration of breast cancer cells.* Mol Cell Biochem, 2020. **465**(1-2): p. 199-214.
45. Carey, R.M., et al., *T2R bitter taste receptors regulate apoptosis and may be associated with survival in head and neck squamous cell carcinoma.* Mol Oncol, 2022. **16**(7): p. 1474-1492.
46. Sessler, D.I., *Long-term consequences of anesthetic management.* Anesthesiology, 2009. **111**(1): p. 1-4.
47. Sheets, M.F., et al., *Sodium channel molecular conformations and antiarrhythmic drug affinity.* Trends Cardiovasc Med, 2010. **20**(1): p. 16-21.
48. Sun, D., Y.C. Li, and X.Y. Zhang, *Lidocaine Promoted Ferroptosis by Targeting miR-382-5p /SLC7A11 Axis in Ovarian and Breast Cancer.* Front Pharmacol, 2021. **12**: p. 681223.
49. Sun, M., S. Huang, and Y. Gao, *Lidocaine inhibits the proliferation and metastasis of epithelial ovarian cancer through the Wnt/beta-catenin pathway.* Transl Cancer Res, 2021. **10**(7): p. 3479-3490.
50. Wall, T.P., et al., *Effects of Lidocaine and Src Inhibition on Metastasis in a Murine Model of Breast Cancer Surgery.* Cancers (Basel), 2019. **11**(10).
51. Sun, H. and Y. Sun, *Lidocaine inhibits proliferation and metastasis of lung cancer cell via regulation of miR-539/EGFR axis.* Artif Cells Nanomed Biotechnol, 2019. **47**(1): p. 2866-2874.
52. Mirshahidi, S., et al., *Bupivacaine and Lidocaine Induce Apoptosis in Osteosarcoma Tumor Cells.* Clin Orthop Relat Res, 2021. **479**(1): p. 180-194.
53. Zhu, J. and S. Han, *Lidocaine inhibits cervical cancer cell proliferation and induces cell apoptosis by modulating the lncRNA-MEG3/miR-421/BTG1 pathway.* Am J Transl Res, 2019. **11**(9): p. 5404-5416.
54. Meyerhof, W., et al., *The molecular receptive ranges of human TAS2R bitter taste receptors.* Chem Senses, 2010. **35**(2): p. 157-70.
55. Christensen, J.N., et al., *Identification of robust reference genes for studies of gene expression in FFPE melanoma samples and melanoma cell lines.* Melanoma Res, 2020. **30**(1): p. 26-38.
56. Palmer, A.E., et al., *Ca2+ indicators based on computationally redesigned calmodulin-peptide pairs.* Chem Biol, 2006. **13**(5): p. 521-30.
57. Odaka, H., et al., *Genetically-encoded yellow fluorescent cAMP indicator with an expanded dynamic range for dual-color imaging.* PLoS One, 2014. **9**(6): p. e100252.
58. Fierro, F., et al., *Inhibiting a promiscuous GPCR: iterative discovery of bitter taste receptor ligands.* bioRxiv, 2022: p. 2022.11.24.517821.
59. Jaggupilli, A., et al., *Analysis of the expression of human bitter taste receptors in extraoral tissues.* Mol Cell Biochem, 2017. **426**(1-2): p. 137-147.
60. Spinelli, K.J. and P.G. Gillespie, *Monitoring intracellular calcium ion dynamics in hair cell populations with Fluo-4 AM.* PLoS One, 2012. **7**(12): p. e51874.
61. Shaik, F.A., A. Jaggupilli, and P. Chelikani, *Highly conserved intracellular H208 residue influences agonist selectivity in bitter taste receptor T2R14.* Biochim Biophys Acta Biomembr, 2019. **1861**(12): p. 183057.
62. Di Virgilio, F., et al., *Extracellular ATP and P2 purinergic signalling in the tumour microenvironment.* Nat Rev Cancer, 2018. **18**(10): p. 601-618.
63. Teng, X., et al., *Lidocaine exerts anticancer activity in bladder cancer by targeting isoprenylcysteine carboxylmethyltransferase (ICMT).* Transl Androl Urol, 2021. **10**(11): p. 4219-4230.
64. Ye, L., et al., *Anti-tumor effects of lidocaine on human gastric cancer cells in vitro.* Bratisl Lek Listy, 2019. **120**(3): p. 212-217.

65. Carey, R.M., et al., *T2R bitter taste receptors regulate apoptosis and may be associated with survival in head and neck squamous cell carcinoma.* Mol Oncol, 2021.
66. Straub, S.G., et al., *Stimulation of insulin secretion by denatonium, one of the most bitter-tasting substances known.* Diabetes, 2003. **52**(2): p. 356-64.
67. Shah, J., E.G. Votta-Velis, and A. Borgeat, *New local anesthetics.* Best Pract Res Clin Anaesthesiol, 2018. **32**(2): p. 179-185.
68. McDonough, R.C., et al., *Targeted Gq-GPCR activation drives ER-dependent calcium oscillations in chondrocytes.* Cell Calcium, 2021. **94**: p. 102363.
69. Wang, Y., et al., *GPCR-induced calcium transients trigger nuclear actin assembly for chromatin dynamics.* Nat Commun, 2019. **10**(1): p. 5271.
70. Chakraborty, S. and G. Hasan, *Store-Operated Ca(2+) Entry in Drosophila Primary Neuronal Cultures.* Methods Mol Biol, 2018. **1843**: p. 125-136.
71. Gruntovskii, G., *[Ceramic plastic repair in treating giant cell bone tumors].* Ortop Travmatol Protez, 1986(8): p. 4-5.
72. Fahrner, M., et al., *The STIM1/Orai signaling machinery.* Channels (Austin), 2013. **7**(5): p. 330-43.
73. Bodnar, D., et al., *STIM-TRP Pathways and Microdomain Organization: Ca(2+) Influx Channels: The Orai-STIM1-TRPC Complexes.* Adv Exp Med Biol, 2017. **993**: p. 139-157.
74. Amran, M.S., N. Homma, and K. Hashimoto, *Pharmacology of KB-R7943: a Na+-Ca2+ exchange inhibitor.* Cardiovasc Drug Rev, 2003. **21**(4): p. 255-76.
75. Zhang, B.X., et al., *Differential regulation of intracellular calcium oscillations by mitochondria and gap junctions.* Cell Biochem Biophys, 2006. **44**(2): p. 187-203.
76. Talmon, M., et al., *Absinthin, an agonist of the bitter taste receptor hTAS2R46, uncovers an ER-to-mitochondria Ca(2+)-shuttling event.* J Biol Chem, 2019. **294**(33): p. 12472-12482.
77. Chung, Y.K. and Y.H. Wong, *Re-examining the 'Dissociation Model' of G protein activation from the perspective of Gbetagamma signaling.* FEBS J, 2021. **288**(8): p. 2490-2501.
78. Lambert, N.A., *Dissociation of heterotrimeric g proteins in cells.* Sci Signal, 2008. **1**(25): p. re5.
79. Kim, D., et al., *Coupling of Airway Smooth Muscle Bitter Taste Receptors to Intracellular Signaling and Relaxation Is via Galphai1,2,3.* Am J Respir Cell Mol Biol, 2017. **56**(6): p. 762-771.
80. Chung, W.C. and J.C. Kermode, *Suramin disrupts receptor-G protein coupling by blocking association of G protein alpha and betagamma subunits.* J Pharmacol Exp Ther, 2005. **313**(1): p. 191-8.
81. Mangmool, S. and H. Kurose, *G(i/o) protein-dependent and -independent actions of Pertussis Toxin (PTX).* Toxins (Basel), 2011. **3**(7): p. 884-99.
82. Uemura, T., et al., *Biological properties of a specific Galpha q/11 inhibitor, YM-254890, on platelet functions and thrombus formation under high-shear stress.* Br J Pharmacol, 2006. **148**(1): p. 61-9.
83. Liu, B. and D. Wu, *Analysis of G protein-mediated activation of phospholipase C in cultured cells.* Methods Mol Biol, 2004. **237**: p. 99-102.
84. Roland, W.S., et al., *6-methoxyflavanones as bitter taste receptor blockers for hTAS2R39.* PLoS One, 2014. **9**(4): p. e94451.
85. Zhou, D., et al., *Repositioning Lidocaine as an Anticancer Drug: The Role Beyond Anesthesia.* Front Cell Dev Biol, 2020. **8**: p. 565.
86. Butler, M., M. Spearman, and K. Braasch, *Monitoring cell growth, viability, and apoptosis.* Methods Mol Biol, 2014. **1104**: p. 169-92.

87. Zhang, B.B., et al., *Mitochondrial membrane potential and reactive oxygen species in cancer stem cells.* Fam Cancer, 2015. **14**(1): p. 19-23.
88. Iijima, T., *Mitochondrial membrane potential and ischemic neuronal death.* Neurosci Res, 2006. **55**(3): p. 234-43.
89. Soutar, M.P.M., et al., *FBS/BSA media concentration determines CCCP's ability to depolarize mitochondria and activate PINK1-PRKN mitophagy.* Autophagy, 2019. **15**(11): p. 2002-2011.
90. Katakam, P.V., et al., *Depolarization of mitochondria in neurons promotes activation of nitric oxide synthase and generation of nitric oxide.* Am J Physiol Heart Circ Physiol, 2016. **310**(9): p. H1097-106.
91. Long, D., et al., *Lidocaine promotes apoptosis in breast cancer cells by affecting VDAC1 expression.* BMC Anesthesiol, 2022. **22**(1): p. 273.
92. Wang, W.Z., et al., *Lidocaine-induced ASC apoptosis (tumescent vs. local anesthesia).* Aesthetic Plast Surg, 2014. **38**(5): p. 1017-23.
93. Zhao, L., et al., *Lidocaine Inhibits Hepatocellular Carcinoma Development by Modulating circ_ITCH/miR-421/CPEB3 Axis.* Dig Dis Sci, 2021. **66**(12): p. 4384-4397.
94. Werdehausen, R., et al., *Lidocaine induces apoptosis via the mitochondrial pathway independently of death receptor signaling.* Anesthesiology, 2007. **107**(1): p. 136-43.
95. Xue, Y. and A.Z. Wang, *DJ-1 plays a neuroprotective role in SH-SY5Y cells by modulating Nrf2 signaling in response to lidocaine-mediated oxidative stress and apoptosis.* Kaohsiung J Med Sci, 2020. **36**(8): p. 630-639.
96. Chang, Y.C., et al., *Local anesthetics induce apoptosis in human thyroid cancer cells through the mitogen-activated protein kinase pathway.* PLoS One, 2014. **9**(2): p. e89563.
97. Kobayashi, K., et al., *Cytotoxicity and type of cell death induced by local anesthetics in human oral normal and tumor cells.* Anticancer Res, 2012. **32**(7): p. 2925-33.
98. Zhu, G., et al., *Differential effects and mechanisms of local anesthetics on esophageal carcinoma cell migration, growth, survival and chemosensitivity.* BMC Anesthesiol, 2020. **20**(1): p. 126.
99. Choudhary, G.S., S. Al-Harbi, and A. Almasan, *Caspase-3 activation is a critical determinant of genotoxic stress-induced apoptosis.* Methods Mol Biol, 2015. **1219**: p. 1-9.
100. Lamkanfi, M. and T.D. Kanneganti, *Caspase-7: a protease involved in apoptosis and inflammation.* Int J Biochem Cell Biol, 2010. **42**(1): p. 21-4.
101. Brentnall, M., et al., *Caspase-9, caspase-3 and caspase-7 have distinct roles during intrinsic apoptosis.* BMC Cell Biol, 2013. **14**: p. 32.
102. Zeng, W., et al., *Lidocaine suppresses the malignant behavior of gastric cancer cells via the c-Met/c-Src pathway.* Exp Ther Med, 2021. **21**(5): p. 424.
103. Tan, Y., et al., *GNB2 is a mediator of lidocaine-induced apoptosis in rat pheochromocytoma PC12 cells.* Neurotoxicology, 2016. **54**: p. 53-64.
104. Villarruel, E.Q., et al., *Lidocaine-induced apoptosis of gingival fibroblasts: participation of cAMP and PKC activity.* Cell Biol Int, 2011. **35**(8): p. 783-8.
105. Gao, J., H. Hu, and X. Wang, *Clinically relevant concentrations of lidocaine inhibit tumor angiogenesis through suppressing VEGF/VEGFR2 signaling.* Cancer Chemother Pharmacol, 2019. **83**(6): p. 1007-1015.
106. Huerta-Bahena, J., R. Villalobos-Molina, and J.A. Garcia-Sainz, *Cycloheximide: an adrenergic agent.* Life Sci, 1982. **30**(20): p. 1757-62.
107. Westra, S.I.P.W.H., *Molecular pathology of head and neck cancer: implications for diagnosis, prognosis, and treatment* Annual Review of Pathology: Mechanisms of Disease, 2009. **4**: p. 49-70.

108. Cramer, J.D., et al., *The changing therapeutic landscape of head and neck cancer.* Nat Rev Clin Oncol, 2019. **16**(11): p. 669-683.
109. Bossola, M., *Nutritional interventions in head and neck cancer patients undergoing chemoradiotherapy: a narrative review.* Nutrients, 2015. **7**(1): p. 265-76.
110. De Felice, F., D. Musio, and V. Tombolini, *Head and neck cancer: metronomic chemotherapy.* BMC Cancer, 2015. **15**: p. 677.
111. Specenier, P.M. and J.B. Vermorken, *Neoadjuvant chemotherapy in head and neck cancer: should it be revisited?* Cancer Lett, 2007. **256**(2): p. 166-77.
112. Concu, R. and M. Cordeiro, *Cetuximab and the Head and Neck Squamous Cell Cancer.* Curr Top Med Chem, 2018. **18**(3): p. 192-198.
113. Mei, Z., et al., *Immune checkpoint pathways in immunotherapy for head and neck squamous cell carcinoma.* Int J Oral Sci, 2020. **12**(1): p. 16.
114. Lu, P., et al., *Extraoral bitter taste receptors in health and disease.* J Gen Physiol, 2017. **149**(2): p. 181-197.
115. Leppert, W., et al., *Transdermal and Topical Drug Administration in the Treatment of Pain.* Molecules, 2018. **23**(3).
116. Pe'er, J., *Ocular surface squamous neoplasia: evidence for topical chemotherapy.* Int Ophthalmol Clin, 2015. **55**(1): p. 9-21.
117. Jain, R., et al., *Nanocarrier Based Topical Drug Delivery- A Promising Strategy for Treatment of Skin Cancer.* Curr Pharm Des, 2020. **26**(36): p. 4615-4623.
118. Gilani, S.J., et al., *Nano-Based Therapy for Treatment of Skin Cancer.* Recent Pat Antiinfect Drug Discov, 2018. **13**(2): p. 151-163.
119. Gutierrez, A., M. Atilhan, and S. Aparicio, *A theoretical study on lidocaine solubility in deep eutectic solvents.* Phys Chem Chem Phys, 2018. **20**(43): p. 27464-27473.
120. Kirkland, D.J., et al., *A weight of evidence assessment of the genotoxicity of 2,6-xylidine based on existing and new data, with relevance to safety of lidocaine exposure.* Regul Toxicol Pharmacol, 2021. **119**: p. 104838.
121. Eberhardt, M., et al., *TRPA1 and TRPV1 are required for lidocaine-evoked calcium influx and neuropeptide release but not cytotoxicity in mouse sensory neurons.* PLoS One, 2017. **12**(11): p. e0188008.
122. Kiss, F., et al., *Transient Receptor Potential (TRP) Channels in Head-and-Neck Squamous Cell Carcinomas: Diagnostic, Prognostic, and Therapeutic Potentials.* Int J Mol Sci, 2020. **21**(17).
123. Chen, T.M., et al., *TRPM7 via calcineurin/NFAT pathway mediates metastasis and chemotherapeutic resistance in head and neck squamous cell carcinoma.* Aging (Albany NY), 2022. **14**(12): p. 5250-5270.
124. Zhao, L.Y., et al., *The overexpressed functional transient receptor potential channel TRPM2 in oral squamous cell carcinoma.* Sci Rep, 2016. **6**: p. 38471.
125. McLaughlin, S.K., et al., *Gustducin and transducin: a tale of two G proteins.* Ciba Found Symp, 1993. **179**: p. 186-96; discussion 196-200.
126. Liu, M., et al., *Denatonium enhanced the tone of denuded rat aorta via bitter taste receptor and phosphodiesterase activation.* Eur J Pharmacol, 2020. **872**: p. 172951.
127. Tietze, D., et al., *Structural and Dynamical Basis of G Protein Inhibition by YM-254890 and FR900359: An Inhibitor in Action.* J Chem Inf Model, 2019. **59**(10): p. 4361-4373.
128. Tizzano, M., et al., *Expression of Galpha14 in sweet-transducing taste cells of the posterior tongue.* BMC Neurosci, 2008. **9**: p. 110.
129. Wang, T., et al., *Measurement of cAMP for Galphas- and Galphai Protein-Coupled Receptors (GPCRs)*, in *Assay Guidance Manual*, S. Markossian, et al., Editors. 2004: Bethesda (MD).

130. Medapati, M.R., et al., *Bitter taste receptor T2R14 detects quorum sensing molecules from cariogenic Streptococcus mutans and mediates innate immune responses in gingival epithelial cells.* FASEB J, 2021. **35**(3): p. e21375.
131. Wall, T.P. and D.J. Buggy, *Perioperative Intravenous Lidocaine and Metastatic Cancer Recurrence - A Narrative Review.* Front Oncol, 2021. **11**: p. 688896.
132. Zhang, C., C. Xie, and Y. Lu, *Local Anesthetic Lidocaine and Cancer: Insight Into Tumor Progression and Recurrence.* Front Oncol, 2021. **11**: p. 669746.
133. Kirtonia, A., et al., *Repurposing of drugs: An attractive pharmacological strategy for cancer therapeutics.* Semin Cancer Biol, 2021. **68**: p. 258-278.
134. Wiese, K.G., et al., *The effect of lidocaine on growth of cells of head and neck squamous cell carcinoma.* J Craniomaxillofac Surg, 1993. **21**(4): p. 157-62.
135. Budihardjo, I., et al., *Biochemical pathways of caspase activation during apoptosis.* Annu Rev Cell Dev Biol, 1999. **15**: p. 269-90.
136. Crowley, L.C. and N.J. Waterhouse, *Detecting Cleaved Caspase-3 in Apoptotic Cells by Flow Cytometry.* Cold Spring Harb Protoc, 2016. **2016**(11).
137. Ennis, H.L. and M. Lubin, *Cycloheximide: Aspects of Inhibition of Protein Synthesis in Mammalian Cells.* Science, 1964. **146**(3650): p. 1474-6.
138. Frasor, J., et al., *Gene expression preferentially regulated by tamoxifen in breast cancer cells and correlations with clinical outcome.* Cancer Res, 2006. **66**(14): p. 7334-40.
139. Nandi, D., et al., *The ubiquitin-proteasome system.* J Biosci, 2006. **31**(1): p. 137-55.
140. Kawahara, H. and H. Yokosawa, *Intracellular calcium mobilization regulates the activity of 26 S proteasome during the metaphase-anaphase transition in the ascidian meiotic cell cycle.* Dev Biol, 1994. **166**(2): p. 623-33.
141. Djakovic, S.N., et al., *Regulation of the proteasome by neuronal activity and calcium/calmodulin-dependent protein kinase II.* J Biol Chem, 2009. **284**(39): p. 26655-65.
142. Park, J.Y., et al., *Calcium-dependent proteasome activation is required for axonal neurofilament degradation.* Neural Regen Res, 2013. **8**(36): p. 3401-9.
143. Lee, D. and J.H. Hong, *Physiological Overview of the Potential Link between the UPS and Ca(2+) Signaling.* Antioxidants (Basel), 2022. **11**(5).
144. Ross, J.M., L. Olson, and G. Coppotelli, *Mitochondrial and Ubiquitin Proteasome System Dysfunction in Ageing and Disease: Two Sides of the Same Coin?* Int J Mol Sci, 2015. **16**(8): p. 19458-76.
145. Eytan, E., et al., *ATP-dependent incorporation of 20S protease into the 26S complex that degrades proteins conjugated to ubiquitin.* Proc Natl Acad Sci U S A, 1989. **86**(20): p. 7751-5.
146. Dahlmann, B., L. Kuehn, and H. Reinauer, *Studies on the activation by ATP of the 26 S proteasome complex from rat skeletal muscle.* Biochem J, 1995. **309 (Pt 1)**: p. 195-202.
147. Brookes, P.S., et al., *Calcium, ATP, and ROS: a mitochondrial love-hate triangle.* Am J Physiol Cell Physiol, 2004. **287**(4): p. C817-33.
148. Sawant, P.D., et al., *Drug release from hydroethanolic gels. Effect of drug's lipophilicity (logP), polymer-drug interactions and solvent lipophilicity.* Int J Pharm, 2010. **396**(1-2): p. 45-52.
149. Bahrudin, U., et al., *Inhibitory effects of local anesthetics on the proteasome and their biological actions.* Sci Rep, 2017. **7**(1): p. 5079.
150. Guo, F., et al., *Crosstalk between cardiomyocytes and noncardiomyocytes is essential to prevent cardiomyocyte apoptosis induced by proteasome inhibition.* Cell Death Dis, 2020. **11**(9): p. 783.
151. Chen, D., et al., *Inhibition of prostate cancer cellular proteasome activity by a pyrrolidine dithiocarbamate-copper complex is associated with suppression of proliferation and induction of apoptosis.* Front Biosci, 2005. **10**: p. 2932-9.

152. Wu, W.K., et al., *Proteasome inhibition: a new therapeutic strategy to cancer treatment.* Cancer Lett, 2010. **293**(1): p. 15-22.
153. Concannon, C.G., et al., *Apoptosis induced by proteasome inhibition in cancer cells: predominant role of the p53/PUMA pathway.* Oncogene, 2007. **26**(12): p. 1681-92.
154. Fricker, L.D., *Proteasome Inhibitor Drugs.* Annu Rev Pharmacol Toxicol, 2020. **60**: p. 457-476.
155. Nunes, A.T. and C.M. Annunziata, *Proteasome inhibitors: structure and function.* Semin Oncol, 2017. **44**(6): p. 377-380.